DESIGN OF A TUBULAR MICROFABRICATED POWER GENERATION SYSTEM FOR HOT EXHAUST STREAMS

S. Masilamani, I. Boniche, C. D. Meyer, R. J. Durscher, D. P. Arnold
Interdisciplinary Microsystems Group, University of Florida, Gainesville, FL 32611, USA
Phone: 1-(352)-392-7657, E-mail: sivam@ufl.edu

Abstract: This paper presents the preliminary design, modeling, and fabrication efforts for a micromachined thermoelectric power generator to be powered by hot exhaust gases from a small heat engine or fuel cell. The proposed tubular generator is envisioned by stacking multiple TE chip modules, each having radially-oriented thermoelements that extend between silicon fin arrays and are supported by a polyimide membrane. A prototype multi-module stack was fabricated and was experimentally shown to sustain a 36 °C temperature difference between the hot and cold sections for an input gas temperature of 120 °C.

Key Words: waste heat power generation, thermoelectric, multi-chip stacking, heat exchangers

1. INTRODUCTION

With the expansion of high functionality wireless portable electronics, there is an increasing need for high energy density portable power sources. A number of power generation schemes are being developed to capitalize on the high energy density of hydrocarbon fuels, including microscale heat engines and various types of fuel cells [1]. The proposed heat engine systems are expected to expel large amounts of hot exhaust gases with significant thermal energy content. If this thermal energy can be recovered and converted via thermoelectric means into electrical power, overall system efficiencies and power densities may increase significantly.

Thermoelectric (TE) devices have been the popular choice for direct energy conversion between thermal and electrical domains for a number of years [2]. They find widespread application owing to their advantages such as absence of moving parts, ease of fabrication, robustness, and reliability. TE devices that utilize thin-film materials are appealing due to their miniaturization potential [3-4] and potential improved performance over bulk TE materials [5].

Previously, deposition and etching techniques of a thin-film TE material namely PbTe were demonstrated by our group [6]. In this work, we show the feasibility of tailoring Si substrates as suitable platforms for TE thin-films to build a micromachined TE power generator that can extract waste heat from engine exhaust.

2. DESIGN OVERVIEW

The design consists of several TE modules stacked in a pipe-like arrangement. In operation, hot gas passes through the center channel creating an inner hot region, whereas the outer region remains close to ambient temperature. Inner and outer heat fins enhance the fluid-solid heat transfer to create a radially-directed temperature gradient across an annular thermopile (Fig. 1). The thermopile has alternating legs (thermo-

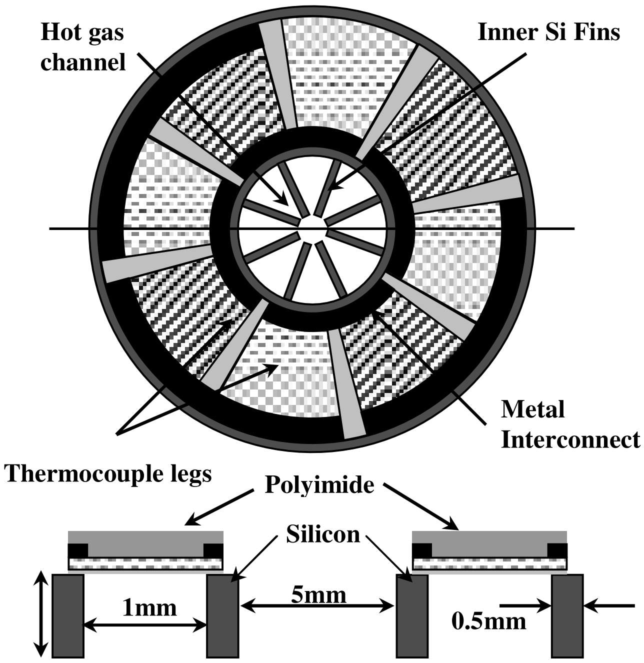

Fig. 1: Top and cross-section views of the proposed unit module with TE elements

elements) of TE material such as a semiconductor and a metal or semiconductors of n- and p-type doping. The silicon underneath the thermopile is etched away to reduce the thermal leakage between the hot and cold sides [7]. A blanket polyimide layer on top of the thermopile provides physical support for the thermoelements, as well as mechanical connection between the inner and outer silicon fin arrays. At the center of each chip module is a circular opening with longitudinal silicon fins. When the modules are stacked (Fig. 2), this forms an internally finned channel for the hot exhaust gas. External annular fins are also formed on the cold side for cross-flow cooling. This is accomplished by making every fourth chip module in the stack to have a larger diameter. The combination of low thermal conductivity polyimide membrane and high thermal conductivity silicon fins is intended to maximize the temperature difference (ΔT) available for power generation.

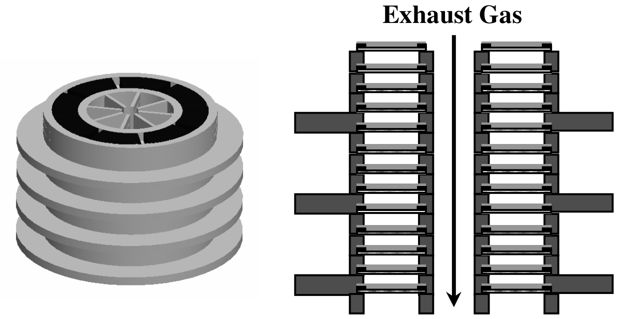

Fig. 2: Stacking of individual TE modules

3. THERMAL MODELING AND DEVICE DESIGN

A simple first-order analytical heat transfer model (Fig. 3) was developed for the individual TE modules assuming 1-D radial heat conduction with convective cooling on the hot and cold sides, and ignoring radiation effects. This model helped guide the design of device parameters such as the diameter of the hot gas channel and heat fin dimensions, as well as the length, thickness, and number of thermocouple legs.

The maximum output power of a TE generator is

$$P_{out} = \frac{V_{oc}^{\ 2}}{4R_{elec}}, \qquad (1)$$

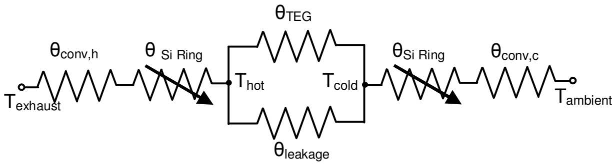

Fig. 3: First-order equivalent thermal circuit of the thermoelectric module.

where R_{elec} is the total electrical resistance of the thermocouple legs and V_{oc} is the generated open circuit voltage for a ΔT temperature difference across the thermocouples. For n thermocouple legs each with a seebeck coefficient of α,

$$V_{oc} = n\alpha\Delta T \,. \qquad (2)$$

In light of these relations, it can be inferred that output power can be increased by improving material properties (α and film resistivity, ρ) or maximizing the thermocouple temperature difference ΔT. Increasing n on other hand is not helpful as it increases both V_{oc}^2 as well as R_{elec}. For a given thermocouple material, α and ρ remain fixed, leaving ΔT as the key variable for maximizing output power.

The thermocouple temperature difference $\Delta T = T_{hot} - T_{cold}$ is a function of thermal resistances [8] (Fig. 3) and the temperature difference between the exhaust gas, $T_{exhaust}$, and ambient, $T_{ambient}$:

$$\Delta T = \frac{\left(\theta_{TEG} \parallel \theta_{leakage}\right)\left(T_{exhaust} - T_{ambient}\right)}{\theta_{convh} + \theta_{convc} + \theta_{TEG} \parallel \theta_{leakage}}, \qquad (3)$$

where θ_{TEG} is the effective thermal resistance of the thermocouple legs, $\theta_{leakage}$ represents the thermal leakage through the thin polyimide layer, and $\theta_{conv,c}$ and $\theta_{conv,h}$ are the thermal resistances representing the convective heat transfer on the cold and hot sides, respectively. The thermal resistances of the Si rings are negligible due to the relatively high thermal conductivity of Si and hence are not included in Eq. 3.

As can be seen, the temperature difference ΔT for a given hot gas temperature, T_{hot} can be maximized by reducing the convective thermal resistances or by increasing θ_{TEG} and $\theta_{leakage}$. However, as an increase in thermal resistance θ_{TEG} also indirectly increases the electrical resistance R_{elec}, maximum ΔT need not necessarily imply maximum P_{out}. Thus, the convective thermal resistances $\theta_{conv,h}$ and $\theta_{conv,c}$ should be minimized to improve ΔT and hence output power without affecting R_{elec}. These resistances are given by

$$\theta_{conv} = \frac{1}{hA_s}, \qquad (4)$$

where h is the convection heat transfer coefficient and A_s is the exposed surface area. The maximum fluidic back pressure on the small combustion engine, the source of exhaust gas, sets the minimum diameter of the inner channel. From experiments on a prototypical model airplane engine, the inner channel diameter was set to 5 mm.

The analytical model was implemented in MATLAB to study trade-offs of the device geometry. Assuming worst case convective heat transfer values ($h = 5 - 10\ \mathrm{W/m^2K}$) and limiting the maximum overall diameter to 13 mm, the results indicated a 1 mm polyimide span to be sufficient for the annular radius of the thermopile. Using heat-transfer correlations for internally finned channels [9], the number of fins on the hot side was chosen as eight and their length as 2.4 mm. The annular outer fin length was chosen as 2 mm to maximize fin surface area while meeting size constraints.

4. DEVICE FABRICATION

Fabrication of a prototype device without the thermoelements was achieved using a two-mask MEMS process (Fig. 4). The process started with a 500-µm thick, double-side-polished, thermally oxidized silicon wafer. A 5 µm thick polyimide layer was used to define annular rings on the top side of the wafer. A buffered oxide etch was used to remove all exposed oxide on the front and back sides. Next, a masking photoresist layer was patterned on the backside using a front-to-back aligner. The wafer was then attached to a handle wafer using photoresist, and deep reactive ion etching (DRIE) is performed on the back-side. This step simultaneously removes the Si underneath the thermopile and forms the fin array for the hot gas channel. Finally, the individual TE modules were released in acetone.

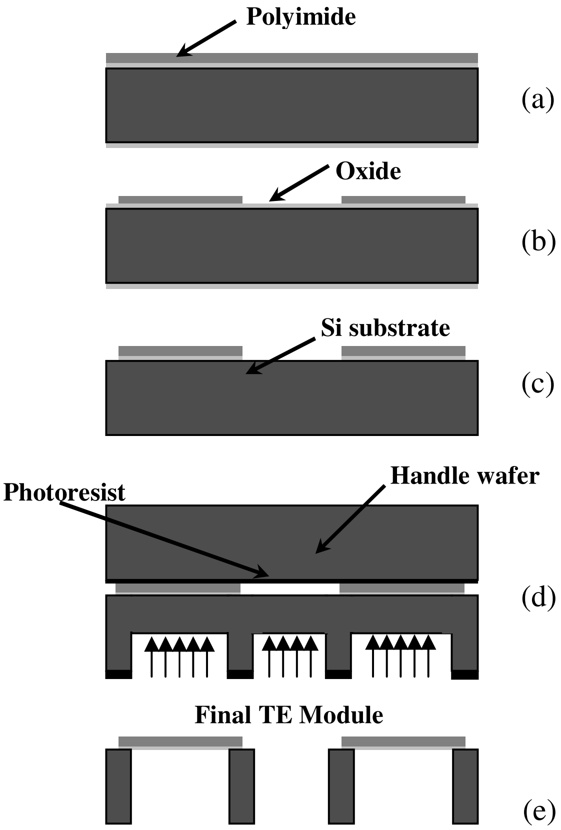

Fig. 4: Prototype device fabrication process flow

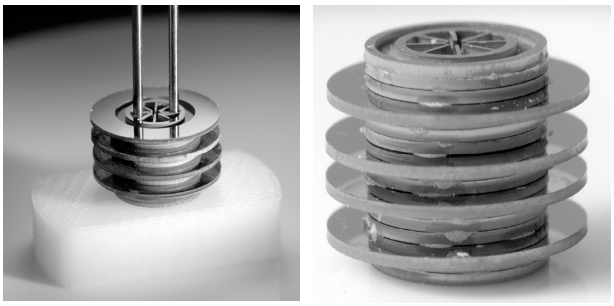

Fig. 5: (a) Setup for stacking the TE modules
(b) Prototype device stack without thermoelements

Stacking of the TE modules was accomplished using an assembly jig with two parallel metal rods (Fig. 5a). The spacing between the rods was made to precisely match the device dimensions. The TE module layers were slid one by one over the alignment rods, and a thermally conductive epoxy was deposited between each layer for bonding. The entire stack was then cured in an oven at 200 °C to yield the final device (Fig. 5b). The overall device dimension was 13 mm in diameter and 8 mm thick.

5. EXPERIMENTAL RESULTS

Experiments (Fig. 6) were performed on the prototype device to characterize the thermal isolation between the inner and outer Si rings and to determine the range of ΔT that can be created across the thermocouple legs. A heat gun provided a constant source of hot gas, and the outer rings were under natural convection. For the experiment, a portion of the outer ring structure was removed to permit access for thermocouple temperature measurements of the inner Si ring. The inner and outer Si ring temperatures are plotted as a function of outlet gas temperature (Fig. 7). A maximum ΔT of 36 ºC was achieved at an outlet gas temperature of around 120 ºC.

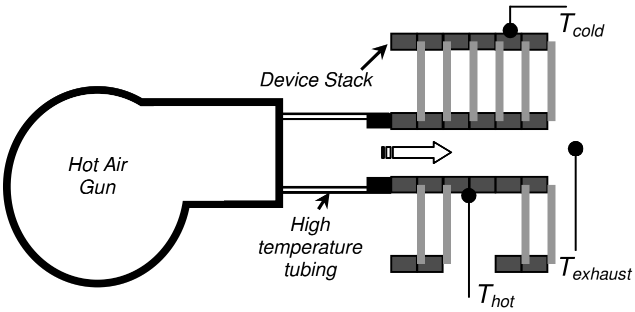

Fig. 6: Schematic of experimental setup

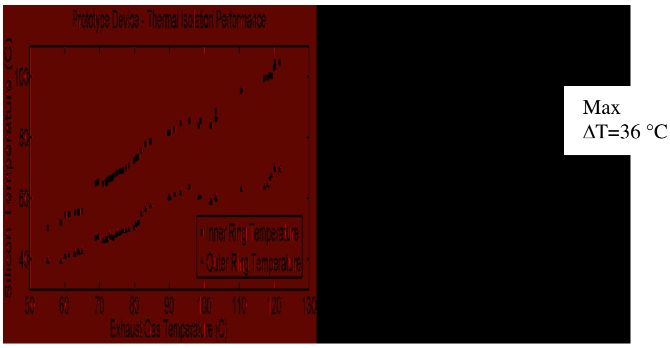

Fig. 7: Plot of inner and outer Si ring temperature vs. exhaust gas temperature

6. CONCLUSION AND FUTURE WORK

The temperature data from the experiment indicates that 36% of the possible 100°C gas-to-ambient temperature difference was achieved, lower than expected. These results indicate the need for better convective heat transfer on the hot and cold sides and/or better thermal isolation. One possible explanation is lateral leakage of hot gas from the channel through the gaps between TE modules. Better bonding methods are being investigated to mitigate this issue. Also, efforts are in progress to integrate the thermoelements to form a prototype TE generator. Clearly, when the thermoelements are introduced into the process flow, additional thermal conduction will occur, resulting in lower ΔT. In summary, the results presented here show the feasibility of the stacked structure fabrication process and provide initial data for feedback into models for improved thermal modeling.

REFERENCES

[1] S. A. Jacobson, A. H. Epstein, An informal survey of Power MEMS, *Proc. Int. Symp. Micro-mechanical Eng.,* Japan, pp. 513-20.

[2] D.M. Rowe, *CRC Handbook of Thermoelectrics*, Boca Raton: CRC Press, 1995.

[3] M. Kishi, H. Nemoto, T. Hamao, M. Yamamoto, S. Sudou, M. Mandai, S. Yamamoto, Micro-Thermoelectric Modules and Their Application to Wrist-watches as an Energy Source, in *Proc. IEEE 18th Int. Conf. Thermoelectrics*, 1999, Baltimore, MD, pp. 301–307.

[4] M. Strasser, R. Aigner, M. Franosch, G. Wachutka, "Miniaturized Thermoelectric Generators Based on Poly-Si and Poly-SiGe Surface Micromachining," *Sensors and Actuators A,* vol. 97-98, pp. 535-542, 2002

[5] R. Venkatasubramanian, E. Siivola, T. Colpitts, B. O'Quinn, Thin film thermoelectric devices with high room-temperature figures of merit, *Nature*, vol. 413, pp. 597-602, 1998.

[6] I. Boniche, C. D. Meyer, P. J. Taylor, N. K. Dhar, D. P. Arnold, Progress towards a Micromachined Thermoelectric Generator using PbTe and PbSnSeTe thin films, in *Tech. Dig. PowerMEMS 2006*, Berkeley, CA, Nov., 2006, pp. 195-198.

[7] S. B. Schaevitz, A. J. Franz, K. F. Jensen, S. J. Schmidt, A Combustion Based MEMS Thermoelectric Generator, *Proc. 11th Int. Conf. Solid State Sensors and Actuators, Munich*, Germany, June 2001, pp. 30-33.

[8] F. Incropera et al, *Fundamentals of Heat and Mass Transfer*, 6th ed., John Wiley & Sons Inc., 2007.

[9] W. Rohsenow et al, *Handbook of Heat Transfer*, 3rd ed., McGraw Hill, 1998.